

# First principles investigation of structural, elastic, electronic and optical properties of Barium seleno-germanate, $\text{Ba}_2\text{GeSe}_4$

Abdu Barde <sup>1,2</sup> and Daniel P Joubert <sup>1</sup>

<sup>1</sup> The National Institute for Theoretical Physics, School of Physics and Mandelstam Institute for Theoretical Physics, University of the Witwatersrand, Johannesburg, Wits 2050, South Africa.

<sup>2</sup> College of Science and Technology, Jigawa state Polytechnic, Dutse - Jigawa state, Nigeria.

E-mail: [abdubarde@gmail.com](mailto:abdubarde@gmail.com)

**Abstract.** Ternary and quaternary chalco-germanates and stannates have a rich structural chemistry. Experimental studies of their non-linear optical properties have been reported, but there are few published computational studies on their structural, elastic, electronic and optical properties. In this work, we investigate the structural, elastic, electronic and optical properties of  $\text{Ba}_2\text{GeSe}_4$  using Density Functional Theory (DFT) and post-DFT many body perturbation theory. The ground state energy and properties, including equilibrium lattice parameters, bulk modulus and band gap were calculated at the DFT level of approximation. The fundamental gap was determined at the post-DFT  $G_0W_0$  level of approximation while optical absorption was determined with the Bether-Salpeter Equation approximation. The ground state energy and mechanical results show that  $\text{Ba}_2\text{GeSe}_4$  is a stable compound while the calculated optical absorption results and estimated optical band gap show that it is a wide band gap material that is well-situated for photon absorption in the high energy visible range with potential application in multi-junction solar cells.

## 1. Introduction

The ternary and quaternary compounds containing metal chalcogenides, chalco-germanates and thio-stannates have received considerable attention due to their structural chemistry [1, 2], important physical and chemical properties for potential applications in non-linear optics (NLO) [3, 4], thin film for solar cell [5] and visible light response photocatalysts [6, 7]. Among the family of chalco-germanates is seleno-germanate earth alkali metal barium seleno-germanate  $\text{Ba}_2\text{GeSe}_4$ . The experimental synthesis of  $\text{Ba}_2\text{GeSe}_4$  has been reported and the compound is found to crystallize in a monoclinic structure with space group  $p12/m$  [8]. The thio/seleno-germanate and stannate compounds exhibit interesting physical properties due their isolated tetrahedral ortho-anion  $[\text{MQ}_4]^{4-}$  corner shearing, where  $[\text{M} = \text{Ge}, \text{Sn}; \text{Q} = \text{S}, \text{Se}]$ . The compounds are well known to have a structure of type  $\text{A}_2\text{MQ}_4$  [4]. Little has been reported on the structural, elastic, electronic and optical properties of  $\text{Ba}_2\text{GeSe}_4$ . We are only aware of the study of Assoud and Soheilnia [8], where the authors reported experimental data on the structure and lattice constants and theoretically investigated the electronic properties using density functional theory with the local density approximation (LDA). However, the authors did not measure the optical band

gap of this compound, but predicted it to lie within 2.6 - 3.0 eV. LDA is well known to give a less accurate description of electronic and optical properties of materials due to the omission of the contribution from quasiparticle renormalization of electronic band gaps and excitonic effect in the linear and non-linear optical absorption [9]. In view of this and the rich range of properties of the seleno-germanate family of compounds with potential practical applications, it is worthy here to investigate the structural, elastic, electronic and optical properties of  $\text{Ba}_2\text{GeSe}_4$ . We use two DFT exchange-correlation approximations, the Perdew-Burke-Ernzerhof generalised gradient approximation (PBE) [10] and PBEsol [11] to determine the ground state energy and lattice structure. DFT band structure calculations were performed using two hybrid functionals, the modified Johnson Becke (MBJ) [12] and Heyd-Scuseria-Ernzerhof (HSE) [13], two approximations that normally improve on the band gap underestimation by local and semi-local DFT approximations. A Green's function (GW) calculation was used to determine the fundamental gap while optical absorption properties were determined within the Bethe-Salpeter Equation (BSE) approximation, which is effective in reproducing the experimental band gap for semiconductors.

## 2. Computational details

The investigation of structural, elastic, electronic and optical properties of  $\text{Ba}_2\text{GeSe}_4$  were carried out within the framework of density functional theory (DFT) as implemented in the Vienna Ab initio simulation package (VASP) [14, 15]. A projected-augmented-wave (PAW) [16] formulation was used for the description of electron-ion interactions. The groundstate energy was calculated within the Perdew-Burke-Ernzerhof generalised gradient approximation (PBE) [10] and PBEsol [11] for the electron exchange correlation relations. Equilibrium structure optimization was performed on the primitive cell of the structure with cut-off energy of 520 eV and a  $6 \times 6 \times 4$  Monkhorst-pack mesh for sampling the Brillouin zone. The k-point mesh sampling was chosen to achieve convergence energies within less than 1 meV/atom. The elastic tensor was calculated for the fully relaxed equilibrium geometry with PBE and PBEsol. DFT band structure calculations were performed for the PBEsol optimized structure using PBEsol and the modified Johnson-Becke potential (MBJ) [12]. The band gap was also estimated with the hybrid Heyd-Scuseria-Ernzerhof (HSE) [13] approximation. The MBJ and HSE approximations normally give a better estimate of the band gap at the DFT level when compared to conventional DFT calculations with local or semi-local exchange-correlation functions. Moreover, in this study we performed a post-DFT many-body Green's function  $G_0W_0$ , [17, 18] calculation to obtain an estimate of the quasi-particle excitations. We used a 180 eV energy cut-off for the response functions to determine the fundamental gap. Finally, the optical absorption spectrum was obtained by including excitonic effects using the  $G_0W_0 + \text{BSE}$  approximation [19, 20, 21]. From the optical absorption spectra, the optical band gap were determined using a Tauc plot [22].

## 3. Result and discussion

### 3.1. Structural properties

X-ray powder diffractogram structural studies reveal that at room temperature the layered ternary  $\text{Ba}_2\text{GeSe}_4$  compound contains isolated tetrahedral  $\text{GeSe}_4$  that form the structure type of  $\text{K}_2\text{ZnBr}_4$ . The compound crystallises in a monoclinic structure, space group  $p2_1/m$  [8], with a conventional unit cell made which contains two  $\text{Ba}_2\text{GeSe}_4$  formula per units cell. Figure 1 shows the  $\text{Ba}_2\text{GeSe}_4$  super cell showing the tetrahedral  $\text{GeSe}_4$  arrangements.

Energy versus volume calculations for  $\text{Ba}_2\text{GeSe}_4$  were performed with the PBE and PBEsol approximations. A 3<sup>rd</sup> order Murnaghan equation of state (EOS) function [23] was fitted to the calculated values and is shown in Fig.2(b). The results show that the PBEsol equilibrium volume is closer to the experimental value than the PBE value. Calculated equilibrium structural parameters and the available experimental data are given in Table.1. Compared to the

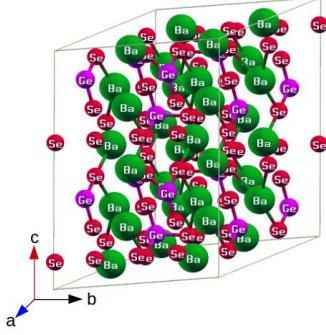


**Figure 1.** Craystal structure of  $\text{Ba}_2\text{GeSe}_4$ .

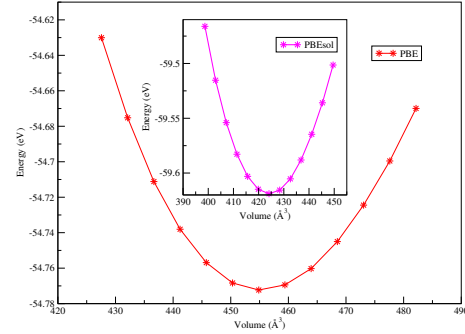


**Figure 2.** Variation of total energy as a function of volume.

experimental data one can clearly see that the calculated lattice parameters ( $a$ ,  $b$  and  $c$ ),  $\beta$ , the angle between cell length  $a$ ,  $b$ , and one of factors that defines the lattice plane spacing, and volume of the unit cell obtained by PBEsol, are very close to the experimentally measured values. The percentage difference of calculated lattice parameter and angle values from experimental values do not exceed 1.54%. Based on the consistent performance of the calculated PBEsol structural parameters, this approximation was used to determine DFT electronic and optical properties and the orresponding calculated structure was used for the GW and BSE calculations.

**Table 1.** Calculated and experimental structural parameters for  $\text{Ba}_2\text{GeSe}_4$ . Lattice parameters  $a$ ,  $b$  and  $c$  in  $\text{Å}$ . The angle between  $a$  and  $b$ ,  $\beta$ , in degrees. Volume  $V$ , in  $\text{Å}^3$ .  $E_{coh}$ , cohesive energy per atom, in eV.

	$a$	$b$	$c$	$V$	$\beta$	$E_{coh}$
PBE	7.204	7.240	9.292	454.96	108.52	-3.61
PBEsol	7.022	6.986	9.150	424.20	109.078	-3.95
Exp.[8]	6.9958	7.0938	9.1738	430.11	109.153	-

### 3.2. Elastic Properties

The elastic properties of a material provides important information about structural stability, binding characteristic, the anisotropy character, the link between mechanical and dynamical properties of a crystal. There are 13 independent elastic constants elastic stiffness constants  $C_{ij}$  for  $\text{Ba}_2\text{GeSe}_4$ , a monoclinic system. The calculated values of the elastic constants, for PBE and PBEsol, satisfy the stability criteria for monoclinic systems [24]. In Table 2 the bulk modulus  $B$ , the shear modulus  $G$ , Young's  $E$  modulus calculated from the  $C_{ij}$  values using the Voigt-Reuss-Hill (VRH) approximation[25, 26] and the ratio  $B/G$ ,  $A^U$ , the universal measure of anisotropy of a material, and the Poisson ratio  $\nu$  of  $\text{Ba}_2\text{GeSe}_4$  are shown. The bulk modulus is a measure of resistance to volume change in response to an applied pressure, while the shear modulus  $G$  is a measure of resistance to reversible deformation due to shear stress. Young's modulus is a measure of resistance to linear stress. Pugh [27] suggested the critical value of 1.75, for  $B/G > 1.75$  the

material behaves in ductile manner otherwise it is brittle. The Voigt and Reuss methods are known to define the upper and lower limits, respectively, of the mechanical parameters. We therefore, use Hill's value which is an arithmetic average of Voigt and Reuss[28] for calculating the values of B/G and  $\nu$ . The determined value of B/G from both PBE and PBEsol indicating that Ba<sub>2</sub>GeSe<sub>4</sub> is ductile material. Similarly,  $\nu$  provides an information of nature in bonding forces and volume compressibility of solid materials,  $\nu$  takes values between  $-1 < \nu < 0.5$ [29]. The determined  $\nu$  for both PBE and PBEsol indicated that Ba<sub>2</sub>GeSe<sub>4</sub> is of good plasticity and have central inter-atomic forces. The calculated bulk modulus at zero pressure, B<sub>0</sub>, from EOS fit, Table 2 and B from VRH approximation are in good agreement demonstrating the reliability of this calculation. The relatively small value of the bulk modulus in Table 2 is evidence that Ba<sub>2</sub>GeSe<sub>4</sub> is not very resistant to volume change with applied pressure. Similarly the values of Young's E is greater than bulk B modulus demonstrating that the title compound is soft material. The departure of  $A^U$  from zero defines the extent of single crystal anisotropy [30].  $A^U$  and the Poisson ratio  $\nu$  were calculated using equations from Ref.[24, 30] which are depicted in Table 2.

**Table 2.** Calculated mechanical parameters. Bulk modulus B<sub>0</sub> and its derivative B'<sub>0</sub> from EOS fitting, bulk B<sub>V</sub>, shear G<sub>H</sub> and Young's E<sub>H</sub> from VRH-approximations modulus in GPa, universal anisotropy  $A^U$ , Poisson's ratio  $\nu$  and ratio B/G of Ba<sub>2</sub>GeSe<sub>4</sub>

	B <sub>0</sub>	B' <sub>0</sub>	B <sub>H</sub>	G <sub>H</sub>	E <sub>H</sub>	$A^U$	$\nu$	B/G
PBE	23.49	6.08	24.44	11.87	30.64	0.939	0.29	2.06
PBEsol	28.01	5.16	26.05	13.29	34.08	1.963	0.28	1.96

### 3.3. Electronic Properties

In Figure 3 and 4 the band structure along the high symmetry directions in the Brillouin zone are shown for PBEsol and the modified Becker Johnson potential (MBJ). MBJ normally gives a better estimation of the gap for large band gap semiconductors. From the band structures for PBEsol and MBJ, Figure 3 and 4 Ba<sub>2</sub>GeSe<sub>4</sub> has a direct band gap of 1.46 eV and 2.26 eV located at  $\Gamma$ , respectively. It is also observed that from the projected density of states (PDOS) that the dominant contributions to the lower conduction band (CB) come from the hybridizations of Se(p), Ge(s) and Ba(d) orbitals, while the upper valency band (VB) is dominated by contributions from Se(p) with a limited contribution from Ba(d) orbitals. Band gaps calculated with PBE, PBEsol, MBJ, HSE and the fundamental gap at the G<sub>0</sub>W<sub>0</sub> level of approximation, are listed in Table 3. The PBE and PBEsol gaps are smaller than the experimental gap, while the MBJ and HSE gaps are closer to the experimental range. The G<sub>0</sub>W<sub>0</sub> estimate of the fundamental gap is smaller than the experimental gap, which is surprising since this estimate is frequently larger than the experimental optical gap.

### 3.4. Optical properties

The study of optical properties gives a better understanding of electronic structure and possible applications of a materials. The frequency dependent dielectric function  $\epsilon(\omega) = \epsilon_1(\omega) + \epsilon_2(\omega)$  fully described the optical properties of a materials [31]. The imaginary part  $\epsilon_2(\omega)$  is obtained from the momentum matrix element between the occupied electronic states relations, while the real part  $\epsilon_1(\omega)$  is determined from the imaginary part through the Kramers-Kronig relations using equations from Ref. [31]. From the calculated structural parameter  $A^U = 1.963$ , Ba<sub>2</sub>GeSe<sub>4</sub> is anisotropic in nature. This is confirmed by the anisotropic nature of its optical properties

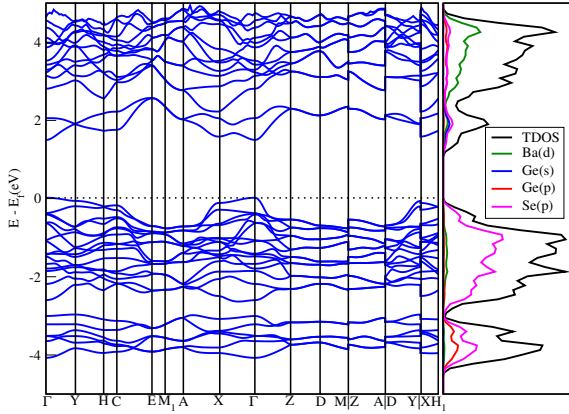


**Figure 3.** PBEsol Electronic bands structure along high symmetry directions

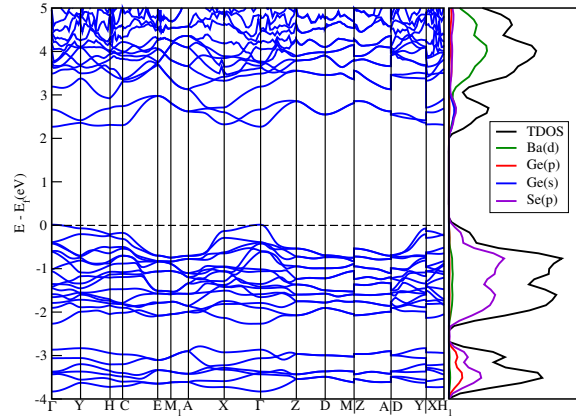


**Figure 4.** MBJ Electronic bands structure along high symmetry directions

**Table 3.** Calculated and experimental band gaps,  $E_g$ , of  $Ba_2GeSe_4$ .

	PBE	PBEsol	MBJ	HSE	$G_0W_0$	Others (LDA)	Exp.
$E_g$ (eV)	1.38	1.46	2.26	2.66	2.53	1.70[8]	2.6 - 3.0 [8]

determined using the  $G_0W_0 + BSE$  calculations. The resolved optical spectra correspond to electric vector polarizations along the x, y and parallel to z directions, respectively. The imaginary part of the dielectric matrix, the optical absorption spectrum and corresponding Tauc plots in the x, y, z directions, are show in Figure 5 and 6. The optical band gap are estimated from Tauc plots with the onset of yy is at 2.05 eV, xx at 2.38 eV and zz at 2.58 eV, which agrees well with the experimental range of 2.6-3.0 eV.

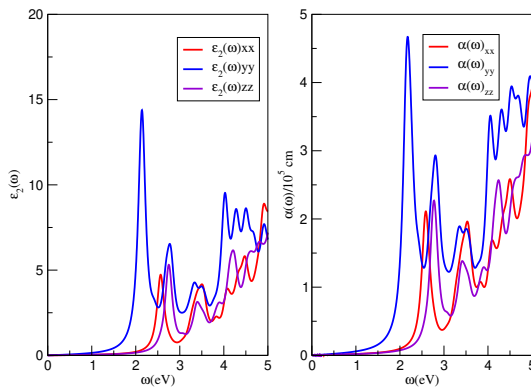


**Figure 5.** The calculated optical functions from left, the imaginary part of the dielectric function, the optical absorption spectra at  $G_0W_0+BSE$  level

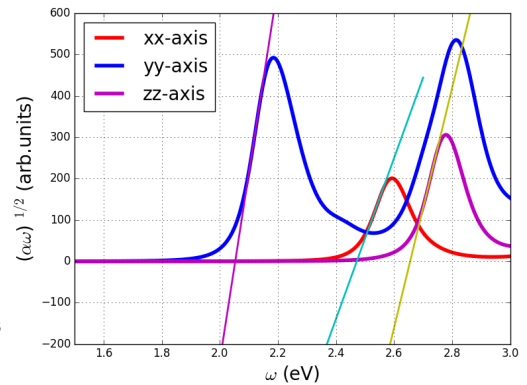


**Figure 6.** The Tauc plot of optical absorption spectra versus photon energy at  $G_0W_0+BSE$  level

### 3.5. Conclusion

Using first principle calculations, we investigate the structural, elastic, electronic and optical properties of the barium seleno-germanate  $\text{Ba}_2\text{GeSe}_4$  compound. The calculated lattice parameters are in reasonable agreement with available experimental data. The electronic band structure calculations from MBJ which provide accurate band structure for most large band gap semiconductors shows an 2.26 eV direct band gap at  $\Gamma - \Gamma$  points other energy gap calculation from HSE and  $G_0W_0$  are within the predicted value. The significant hybridization of Ba(d), Ge(s) and Se(p) was observed from the PDOS analysis of conduction band indicating covalent character in addition to ionic character. The calculated optical properties shows anisotropy. The optical gap are in energetic order of  $yy < xx < zz$ , the onset of  $yy$  is at 2.05 eV,  $xx$  at 2.38 eV and  $zz$  at 2.58 eV, which agreed well with predicted value of 2.6-3.0 eV [8]. Our result shows that  $\text{Ba}_2\text{GeSe}_4$  potential as wide band gap material [32] with potential applications in multi-junction solar cells. [33].

### 3.6. Acknowledgments

The support of Tertiary education trust fund (TET-fund), Nigeria toward this research is here by acknowledged. We highly acknowledged the centre for high performing computing, South-Africa for providing us with computing facilities.

## References

- [1] Wachhold M and Kanatzidis M G 1999 *Inorg. Chem.* **38** 4178–4180
- [2] Sheldrick W S and Wachhold M 1998 *Coord. Chem. Rev.* **176** 211–322
- [3] Mei D, Yin W, Feng K, Lin Z, Bai L, Yao J and Wu Y 2011 *Inorg. Chem.* **51** 1035–1040
- [4] Wu K, Su X, Yang Z and Pan S 2015 *Dalton Trans.* **44** 19856–19864
- [5] Scragg J J et al 2013 *Chem. Mater.* **25** 3162–3171
- [6] Regulacio M D and Han M Y 2016 *Acc. Chem. Res.* **49** 511–519
- [7] Zhou M, Xiao K, Jiang J, Huang H, Lin Z, Yao J and Wu Y 2016 *Inorg. Chem.* **55** 12783–12790
- [8] Assoud A, Soheilnia N and Kleinke H 2004 *Zeitschrift für Naturforschung B* **59** 975–979
- [9] Yakovkin I and Dowben P A 2007 *Surf. Rev. Lett.* **14** 481–487
- [10] Perdew J P, Burke K and Ernzerhof M 1996 *Phys. Rev. Lett.* **77** 3865
- [11] Perdew J P et al 2008 *Phys. Rev. Lett.* **100** 136406
- [12] Tran F and Blaha P 2009 *Phys. Rev. Lett.* **102** 226401
- [13] Heyd J, Scuseria G E and Ernzerhof M 2003 *J. Chem. Phys.* **118** 8207–8215.
- [14] Kresse G and Hafner J 1993 *Phys. Rev. B* **47** 558
- [15] Kresse G and Furthmüller J 1996 *Comput. Mater. Sci.* **6** 15–50
- [16] Kresse G and Joubert D 1999 *Phys. Rev. B* **59** 1758
- [17] Hedin L 1965 *Phys. Rev.* **139** A796
- [18] Hybertsen M S and Louie S G 1986 *Phys. Rev. B* **34** 5390
- [19] Onida G, Reining L and Rubio A 2002 *Rev. Mod. Phys.* **74** 601
- [20] Hanke W and Sham L J 1980 *Phys. Rev. B* **21** 4656
- [21] Salpeter E E and Bethe H A 1951 *Phys. Rev.* **84** 1232
- [22] Tauc J, Grigorovici R and Vancu A 1966 *phys. Stat. Sol. b* **30** 244–247
- [23] Murnaghan F D 1944 *Proc. Natl. Acad. Sci.* **30** 244–247
- [24] Wu Z, Zhao E, Xiang H, Hao X, Liu X and Meng J 2007 *Phys. Rev. B* **76** 054115
- [25] Reuss A 1929 *J. Appl. Math. Mech.* **9** 49–58
- [26] Hill R 1952 *Proc. Phys. Soc. Sec. A* **65** 349
- [27] Pugh S F 1954 *Phil. Mag.* **45** 823–843
- [28] Hirsekorn S 1990 *Text. Stress, Micro.* **12** 1–14
- [29] Boucetta S 2014 *J. Mag. Allo.* **2** 59–63
- [30] Ranganathan S I and Ostojia-Starzewski M 2008 *Phys. Rev. Lett.* **101** 055504
- [31] Saha S, Sinha T P and Mookerjee A 2000 *Phys. Rev. B* **62** 8828
- [32] Yoshikawa A, Matsunami H and Nanishi Y 2007 *Wide Bandgap Semiconductors* (Berlin: Springer)
- [33] Green M A 2003 *Third generation concepts for photovoltaics* (IEEE: 3rd World Conference on Photovoltaic Energy Conversion, Proceedings of)